SPECTROSCOPIC LINE SHAPE STUDIES FOR ENVIRONMENTAL AND METROLOGIC APPLICATIONS

Adriana Predoi-Cross

Department of Physics and Astronomy, University of Lethbridge, Lethbridge AB Canada

OUTLINE OF MY PRESENTATION

- Research Context
- Experimental Setups
- Theoretical Details
- Laser Spectroscopic Studies
- Synchrotron Based Fourier Transfer Spectroscopic Studies
- Metrologic Applications
- References
- Conclusion and Directions for Future Work

Research Context

- High-resolution laboratory molecular spectroscopy is an area of physical sciences that is often used to obtain precise information on molecular species located in areas that are not directly accessible to us, such as high altitude layers of the Earth' atmosphere, planetary atmospheres, or the interstellar space.
- Extremely precise spectral measurements of a line shape can help us both to understand fundamental processes of molecular dynamics and to interpret remote sensing data. Combining the results of laboratory studies and from theoretical models with results from remote sensing measurements, it is possible to determine the chemical composition and physical properties of the remote environments. This is the basis of spectroscopic remote sensing, a technique that is widely used in planetary exploration.
- Science Advisory Groups for spectroscopic remote sensing missions have strongly recommended that new laboratory studies using the best experimental techniques and/or sophisticated theoretical models are required, to enable accurate retrievals of concentration profiles for trace atmospheric constituents.

Objectives For Our Spectrocopic Studies

- The accuracy of atmospheric retrievals can be improved to such a level of accuracy by understanding and removing the sources of systematic errors in the forward model calculations related to spectral line parameters.
- The ultimate question for which we wish to seek answers through this study is "What is it that we are missing in the spectral characterization of atmospheric trace gases to be able to fully and accurately characterize the atmospheric spectrum?"
- We believe the problems may be caused by inadequate molecular line shapes and therefore should carefully examine the appropriate line shape profiles and include line mixing effects.

Experimental Setup @ UofL
3 channel laser spectrometer

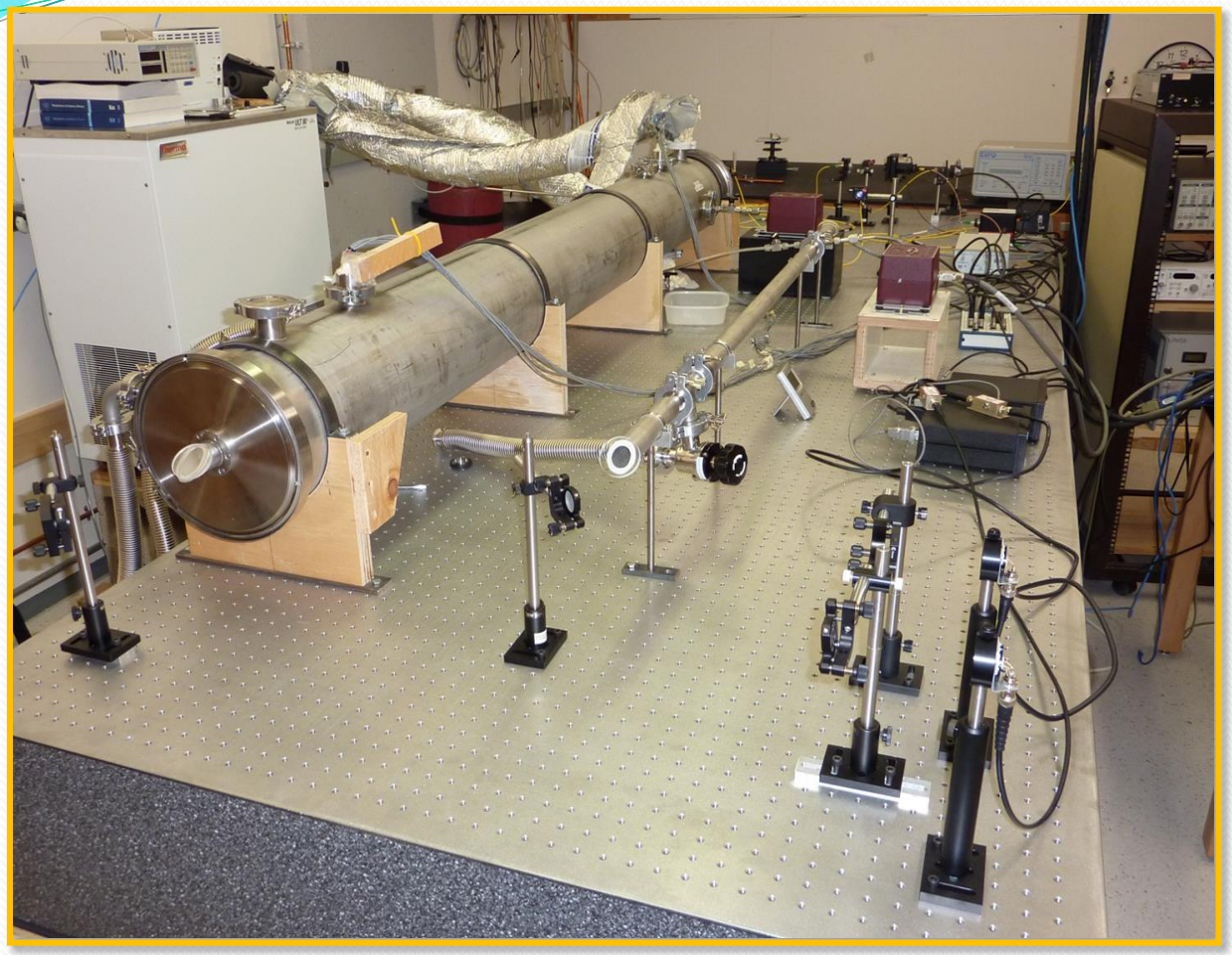

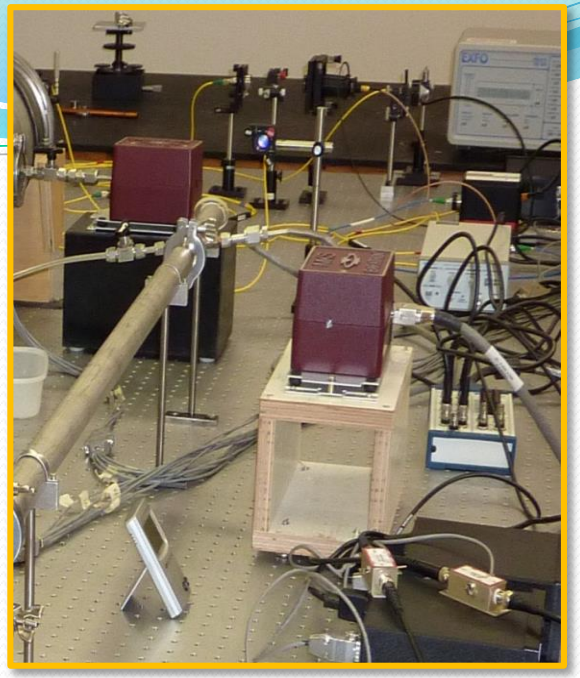

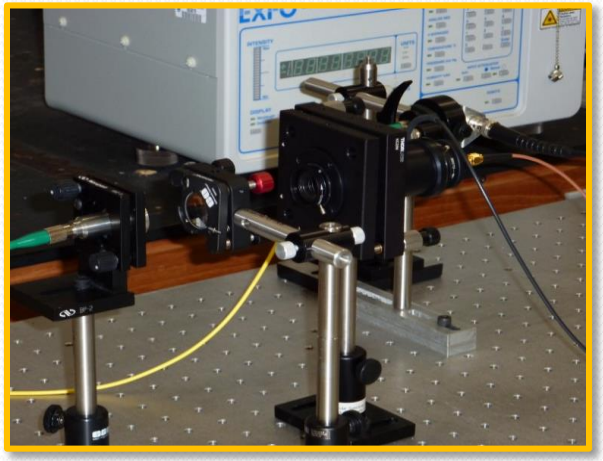

A 3-channel home-made laser spectrometer, tuneable from 1.48 to 3.8 micrometers and several laser sources are available. A variable-temperature single-pass absorption gas cell was custom designed and built for the spectroscopic study of gases. A second room-temperature gas cell is available.

Experimental Setup @ The Far-Infrared Beamline

Canadian Light Source, Saskatoon

CLS Parameters

Energy: 2.9 GeV

Current: 200 mA

Circumference: 171 m, 12 straight sections, 5.2 m long

RF: 500 MHz, 2.4 MV, supercon

Injection: 250 MeV LINAC, full energy booster ring

Main building: ~ 85 x 85 m

Beamsplitter	Spectral Range
Mylar 6 µm	30-630 cm^{-1}
Mylar 75 µm	12-35 cm^{-1}
Ge/KBr	400-4800 cm^{-1}
CaF_2	1850-20000cm^{-1}
Detectors	
MCT N	600-10000 cm^{-1}
MCT B	450-10000 cm^{-1}
DTGS	100-3000 cm^{-1}
DTGS PE	15-700 cm^{-1}
Si Bolometer	10-370 cm^{-1}
Ge:Cu	300-1850 cm^{-1}
Internal Sources	
Globar	10 – 13000 cm^{-1}
Hg – Lamp	10 – 1000 cm^{-1}
Tungsten Lamp	1000-25000cm^{-1}

Optical Element	Label	Optical Element	Label	Optical
Plane	DW	Window	M5	Plane
Ellipsoid	M3	Plane	T2	Cu Target
Cu Target	M4	Ellipsoid	M6	Ellipsoid
			M7	Plane

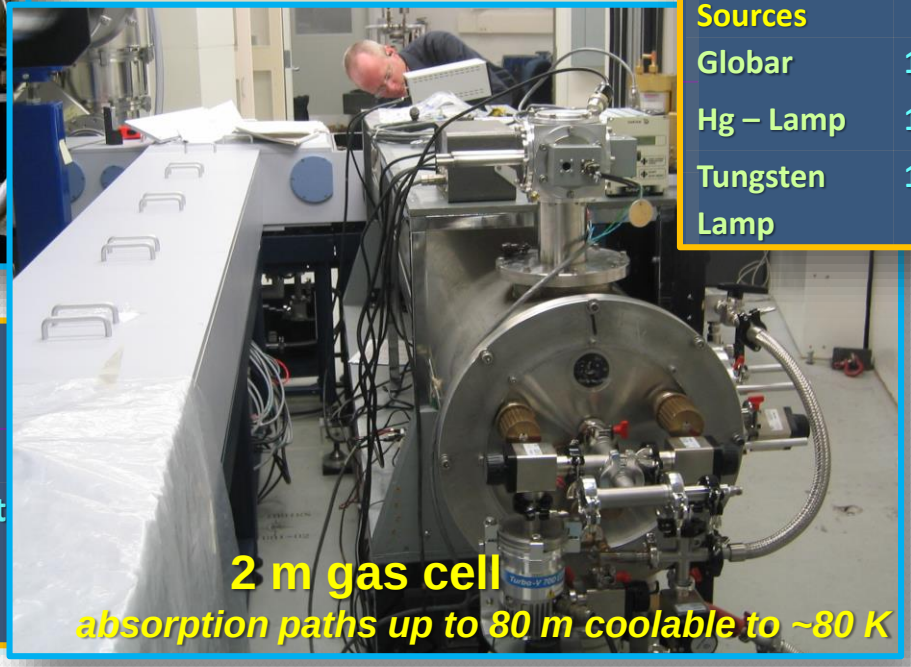

2 m gas cell

absorption paths up to 80 m coolable to ~80 K

Molecular Gas Metrology

- Spectroscopic studies of atmospheric greenhouse gases
- Doppler width thermometry and Boltzmann constant determination
- Verification of fundamental theories of interaction in molecular systems
- New spectroscopic data bases for atmospheric, medical and industrial applications

Spectral line shapes theory

- Ab initio spectral line shape calculation
- Semianalytical line shape models
- Dicke narrowing and speed-dependent effects

Source: Roman Ciurylo, personal communication

Speed-dependent Voigt profile

Berman, *J. Quant. Spectrosc. Radiat. Transf.* **12**, 1331 (1972)

$$I(\omega) = \frac{1}{\pi}\int d^3\vec{v}_a \; f_{m_a}(\vec{v}_a)\,\frac{\Gamma(v_a)}{[\omega-\omega_0-\vec{k}\cdot\vec{v}_a-\Delta(v_a)]^2+\Gamma^2(v_a)}$$

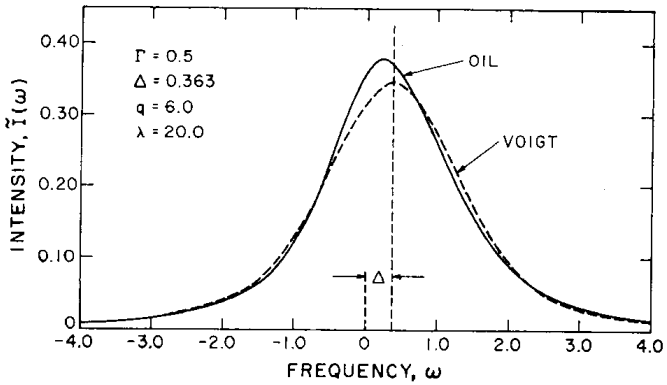

Fig. 2. Comparison of Voigt and model CFA–OIL profiles for non-vanishing shift.

Ward, Cooper, Smith, *J. Quant. Spectrosc. Radiat. Transf.* **14**, 555 (1974)

In molecules:

Ritter, Wilkerson, J. Mol. Spectrosc. 121, 1 (1987)
Farrow, Rahn, Sitz, Rosasco, *Phys. Rev. Lett.* **63**, 746 (1989)
Rohart, Mäder, Nicolaisen, *J. Chem. Phys.* **101**, 6475 (1994)

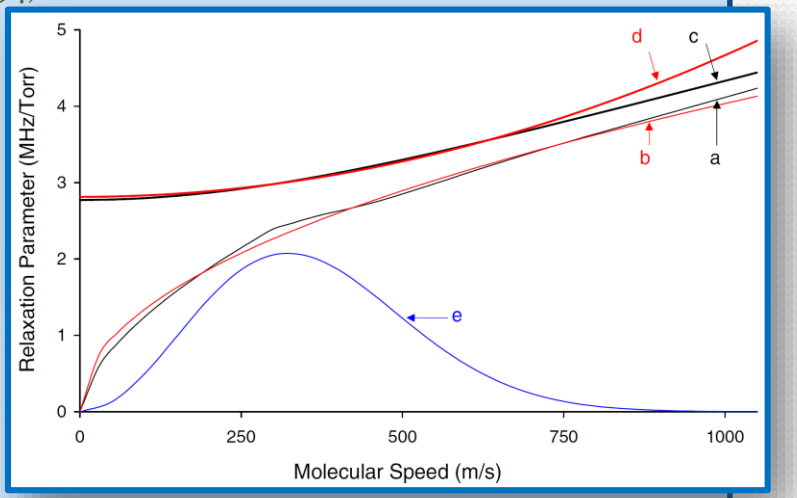

Rohart, Wlodarczak, Colmont, Cazzoli, Dore, Puzzarini, *J. Mol. Spectrosc.* **251**, 282 (2008)

Source: Roman Ciurylo, personal communication

Dicke Narrowing

Dicke, *Phys. Rev.* **89**, 472 (1953)

$$\nu = \frac{k_B T}{m_a D}$$

$$I(\omega) = \frac{1}{\pi} \frac{\omega_D^2/(2\nu)}{\left[\omega - \omega_0\right]^2 + \left[\omega_D^2/(2\nu)\right]^2}$$

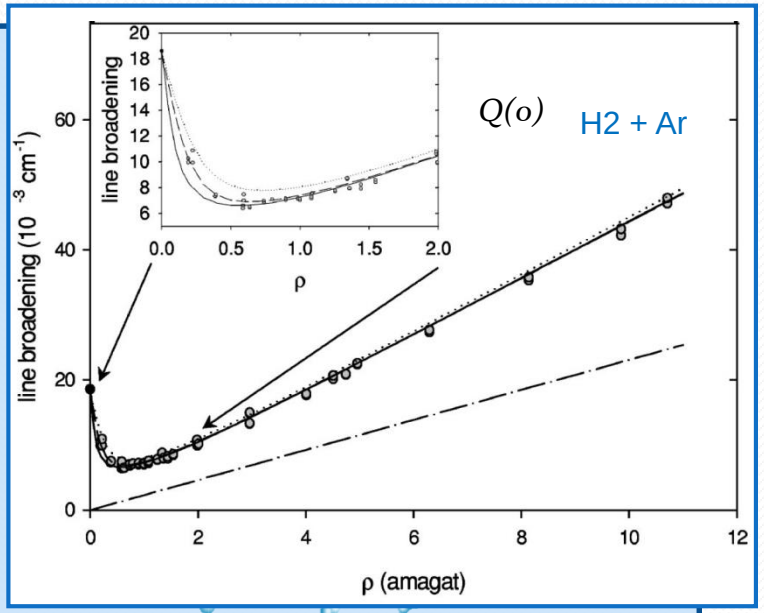

Joubert et al., *Phys. Rev. A* **66**, 042508 (2002)

$$I(\omega) = \frac{1}{\pi} \mathrm{Re} \int_0^\infty dt \int d^3\vec{v} \int d^3\vec{r} \exp\left[i(\omega - \omega_0)t - i\vec{k}\cdot\vec{r}\right] f(\vec{r},\vec{v},t)$$

$$\frac{\partial}{\partial t} f(\vec{r},\vec{v},t) = -\vec{v}\cdot\vec{\nabla}_r f(\vec{r},\vec{v},t) + \hat{S}f(\vec{r},\vec{v},t) \qquad f(\vec{r},\vec{v},0) = \delta^3(\vec{r})\, f_{m_a}(\vec{v})$$

soft and hard

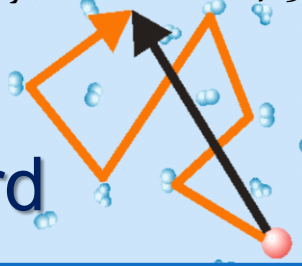

$$\hat{S}f(\vec{r},\vec{v},t) = \nu\vec{\nabla}_v\cdot\left[\vec{v}f(\vec{r},\vec{v},t)\right] + \nu\frac{v_m^2}{2}\Delta_v f(\vec{r},\vec{v},t)$$

GP Galatry, *Phys. Rev.* **122**, 1218 (1961)

$$\hat{S}f(\vec{r},\vec{v},t) = -\nu\, f(\vec{r},\vec{v},t) + \nu\, f_m(\vec{v}) \int d^3\vec{v}'\, f(\vec{r},\vec{v}',t)$$

NGP Nelkin, Ghatak, *Phys. Rev.* **135**, A4 (1964)

collisions

light perturbers

Rautian , Sobelman, *Usp. Fiz. Nauk* **90**, 209 (1966) [*Sov. Phys. Usp.* **9**, 701 (1967)]

not heavy perturbers

RSP

Source: Roman Ciurylo, personal communication

Speed-dependence and Dicke narrowing

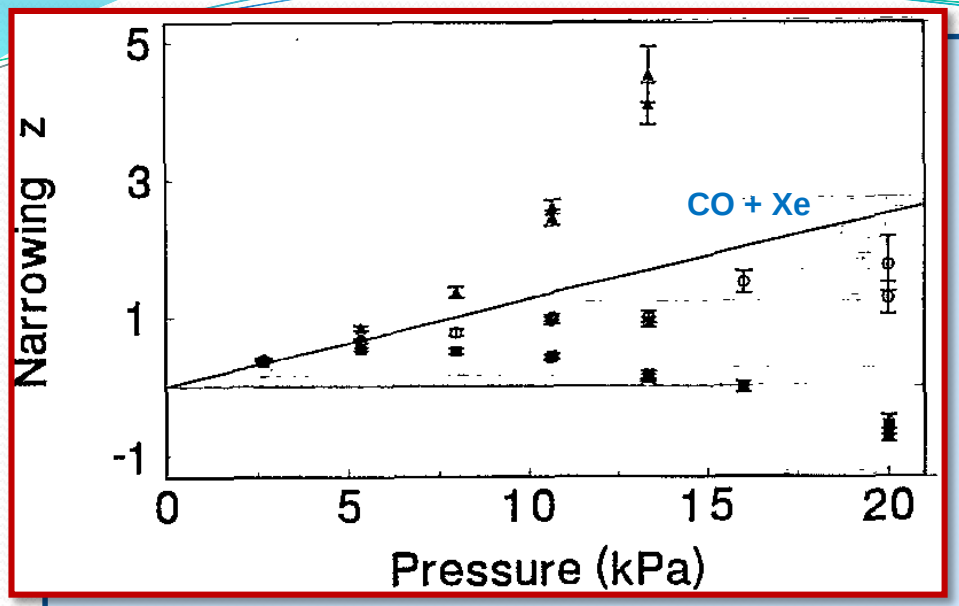

Duggan et al., *Phys. Rev. A* **51**, 218 (1995)

Henry et al., *J. Quant. Spectrosc. Radiat. Transf.* **56**, 647 (1996)

(SDNGP)
speed-dependent Nelkin-Ghatak profile
Lance et al., *J. Mol. Spectrosc.* **185**, 262 (1997)

Duggan et al., *J. Mol. Spectrosc.* **186**, 90 (1997)

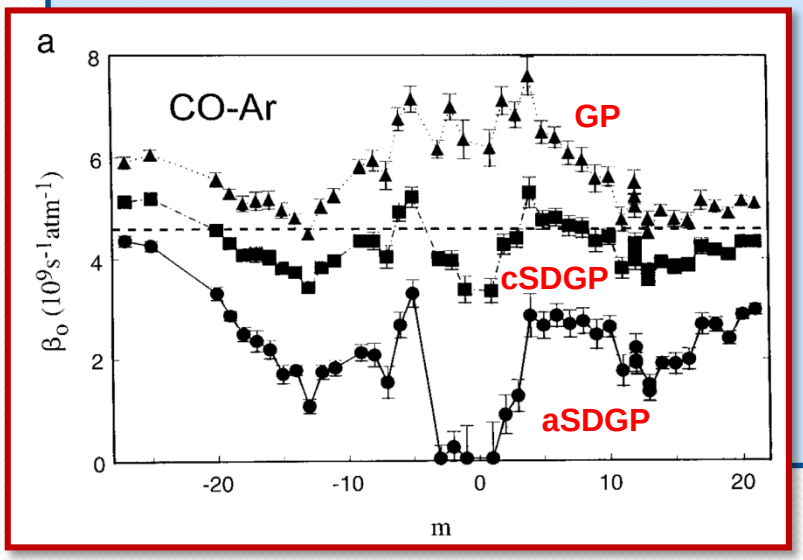

Diffusion

(aSDGP)
approximated **speed-dependent Galatry profile**
Ciuryło, Szudy, *J. Quant. Spectrosc. Radiat. Transf.* **57**, 411 (1997)

Source: Roman Ciurylo, personal communication

Analysis Details

- **Wavenumber scales of all spectra recorded with the laser spectrometer were self-calibrated using line positions recorded on channel 2. The wavenumber scales of the synchrotron based Fourier transform spectra of our spectrometer were recorded using line positions in the HITRAN2012 database.**
- **The interactive multispectrum nonlinear least squares fitting technique (implementation of Hurtmans *et al*. (2002) or Benner *et al.* (1995)) was used to analyze limited wavenumber intervals of all spectra recorded in a given experiment, simultaneously.**
- **Different line shape profiles were assumed. Including speed-dependence in our spectral profiles did improve the fit residuals (observed-calculated).**
- **Line mixing was necessary to accurately model the absorption.**
- **Initial values for all line parameters were taken from the HITRAN2012 database. The pressure-shift coefficients had initial values of zero, and an initial value of 0.7 was assumed for all temperature-dependence exponents of broadening coefficients.**
- **Spectral backgrounds (including some channeling), zero transmission levels, instrument line shapes were appropriately modeled.**

Expressions for Broadening and Shift Parameters

$$b_L(p,T) = p\left[b_L^0(N_2)(p_0,T_0)(1-\chi)\left[\frac{T_0}{T}\right]^{n1} + b_L^0(self)(p_0,T_0)\chi\left[\frac{T_0}{T}\right]^{n2}\right]$$

Where $b_L(p,T)$ is the Lorentz halfwidth (in cm^{-1}) of the spectral line at pressure p and temperature T, and the broadening coefficient $b_L^0(Gas)(p_0,T_0)$ is the Lorentz halfwidth of the line at the reference pressure p_0 (1 atm) and temperature T_0(296 K), and χ is the ratio of the partial pressure of acetylene to the total sample pressure in the cell. The temperature dependence exponents of the pressure-broadening coefficients are *n1* and *n2*.

$$\nu = \nu_0 + p\left[\delta^0(N_2)(1-\chi) + \delta^0(self)\chi\right]$$

Where ν_0 is the zero-pressure line position (in cm^{-1}), ν is the line position corresponding to the pressure p, δ^0 is the pressure-induced line shift coefficient at the reference pressure p_0*(1 atm)* and temperature T_0*(296 K)* of the broadening gas (foreign broadener or self), and χ is as defined above.

$$\delta^0(T) = \delta^0(T_0) + \delta'(T - T_0).$$

The temperature dependence of the pressure induced shift coefficient (in $cm^{-1}atm^{-1}K^{-1}$) is δ'. $\delta^0(T)$ and $\delta^0(T_0)$ represent the pressure induced shift coefficients (in cm^{-1} atm^{-1}) at T and T_0 *(296 K)*, respectively. An initial estimate of zero was assumed for δ' for both foreign- and self-broadening.

Synchrotron Based Spectroscopic Studies of Atmospheric Trace Constituents (Ammonia, Formic Acid, Methanol,..)

(A) The spectrum of $^{15}NH_3$ in the 66-2000 cm^{-1} region

A. Predoi-Cross[a], H. Rozario[a], M. Herman[b], E. Cané[c], G. Di Lonardo[c], L. Fusina[c]

[a]*Department of Physics and Astronomy, University of Lethbridge, Lethbridge Canada;* [b]*Laboratoire de Chimie Quantique et Photophysique, Université Libre de Bruxelles, Bruxelles, Belgium;* [c]*Dipartimento di Chimica Industriale "Toso Montanari", Università di Bologna, Viale Risorgimento 40136 Bologna, Italy*

- Ammonia is a well studied molecule owing to its importance as a model molecule possessing internal inversion motion which can be characterized by infrared spectroscopy.
- Among the isotopically substituted molecules, $^{15}NH_3$ received little attention in comparison with the parent main isotope $^{14}NH_3$. $^{15}NH_3$ has an energy pattern very similar to that of $^{14}NH_3$ and represents a suitable test to check the assignment of the transitions and the adequacy of the Hamiltonian for the description of the spectrum, in particular at very high J values.
- While recently the ground state transitions of $^{14}NH_3$ [1] has been reinvestigated by means of several high resolution techniques, only two studies were devoted to the analogous spectra in $^{15}NH_3$ [2,3]. Of these, the most recent was performed in 1994 and rotation-inversion transitions were measured only up to J = 6. The bending states of $^{15}NH_3$ were also analysed using spectra recorded at moderate resolution [4].

Spectroscopic Goals for this study

- The use of infrared techniques to retrieved tropospheric species is a very powerful technique, provided that accurate spectroscopic parameters are used to analyze the observed spectra.
- The goal of the present study is to perform the first detailed infrared study of $^{15}NH_3$ in the far-infrared region. The target task, in the near future, will be to provide a precise and consistent list of $^{15}NH_3$ lines involving accurate line position, intensity and air-broadening parameters.
- Since the knowledge of the ground state energy pattern is essential to investigate the vibrationally excited states we recorded the far infrared spectrum of the molecule at very high resolution and path length in order to observe very high J transitions and also the rotation-inversion spectrum in the lowest excited vibrational states.
- We aimed to observe perturbation allowed transitions, which are essential to better characterize the rotation and distortion parameters related to the axis of symmetry, C, D_K, H_K, … .
- The spectral range investigated extends from 60 to 2000 cm^{-1} allowing the observation of transitions $\nu_2 \leftarrow$ GS, $\nu_4 \leftarrow$ GS, $2\nu_2 \leftarrow$ GS and the hot bands $2\nu_2 \leftarrow \nu_2$, $\nu_4 \leftarrow \nu_2$ and $2\nu_2 \leftarrow \nu_4$.

The Inversion Motion of Ammonia Molecule

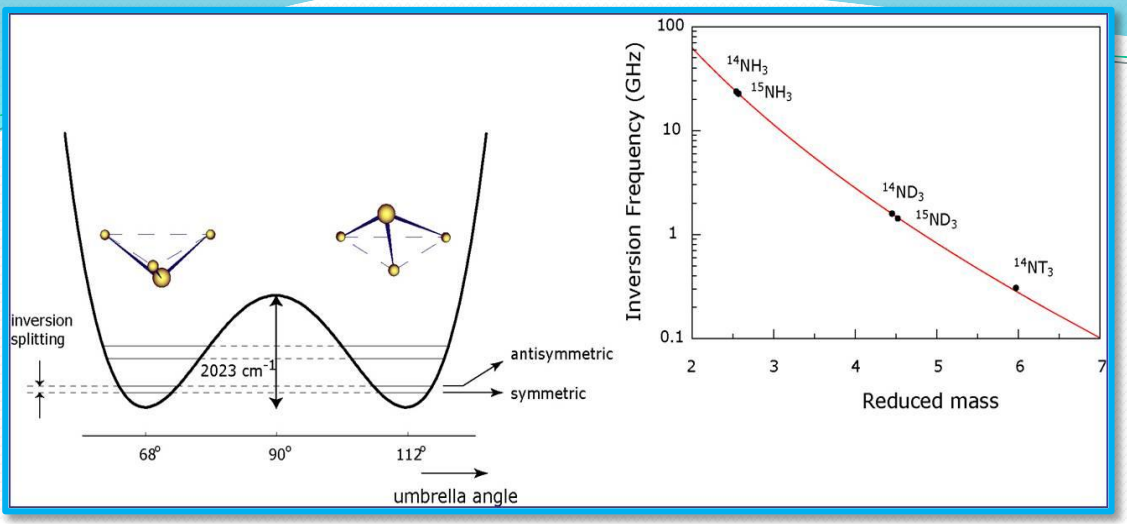

$^{15}NH_3$

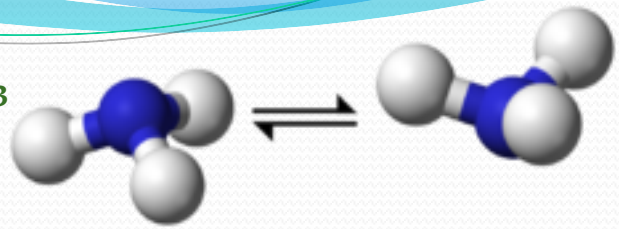

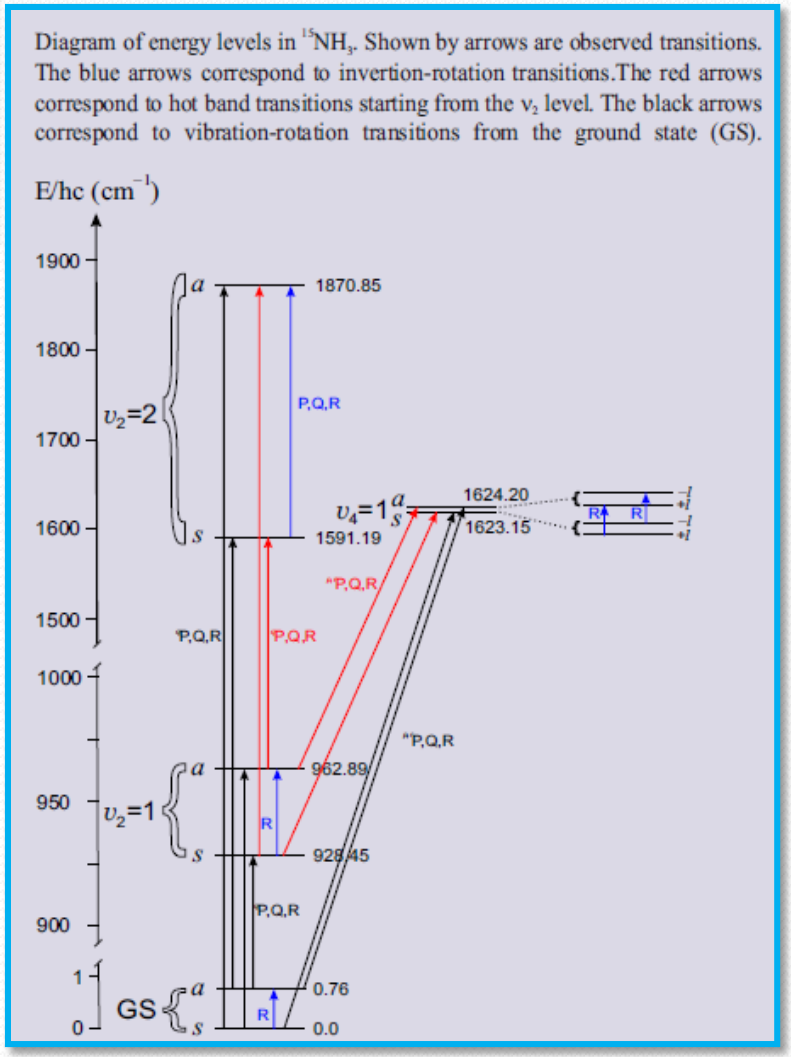

- The N atom can tunnel quantum mechanically through the plane of the H atoms. The potential barrier due to the H atoms is low enough that such tunneling occurs rapidly, resulting in the two lowest vibrational states providing a transition frequency that falls in the microwave range.
- All (J, K) rotational states are thus split into *inversion doublets* (except for K = o, where nuclear spin statistics and symmetry considerations eliminate half of the inversion doublet). The ΔJ=0, ΔK=0 inversion transitions across the doublets are allowed from symmetry considerations (Townes & Schawlow 1 955). The inversion doublets are further split by hyperfine interactions.

Source: P.T. Ho, C. Townes, Ann. Rev. Astron. Astrophys. 1983. 21: 239-70

Spectroscopic Analysis Of $^{15}NH_3$ Spectrum Below 2000 cm^{-1}

we report on the observation and the analysis of the inversion rotation spectrum in the ground, v_2 = 1, v_4=1 and v_2 = 2 states. All the allowed and forbidden inversion-rotation transitions belonging to the ground state, together with transitions present in the literature, were fitted simultaneously on the basis of an inversion-rotational Hamiltonian. 651 transitions with *J* up to 23 were fitted to 54 parameters, with a RMS value for 534 FIR lines of 0.98×10-4 cm-1 (3.3 MHz).

Molecular Hamiltonian for the ground state containing diagonal, and ΔK=±3, 6 off-diagonal terms.

$$
\begin{aligned}
{}^{(i)}E(J,K) = {}&{}^{(i)}E^0 + {}^{(i)}B\left[J(J+1)-K^2\right] + {}^{(i)}CK^2 - {}^{(i)}D_J\left[J(J+1)\right]^2 - {}^{(i)}D_{JK}\left[J(J+1)\right]K^2 - {}^{(i)}D_K K^4 \\
&+ {}^{(i)}H_J\left[J(J+1)\right]^3 + {}^{(i)}H_{JJK}\left[J(J+1)\right]^2 K^2 + {}^{(i)}H_{JKK}\left[J(J+1)\right]K^4 + {}^{(i)}H_K K^6 \\
&+ {}^{(i)}L_J\left[J(J+1)\right]^4 + {}^{(i)}L_{JJJK}\left[J(J+1)\right]^3 K^2 + {}^{(i)}L_{JJKK}\left[J(J+1)\right]^2 K^4 + {}^{(i)}L_{JKKK}\left[J(J+1)\right]K^6 + {}^{(i)}L_K K^8 \\
&+ {}^{(i)}M_J\left[J(J+1)\right]^5 + {}^{(i)}M_{JJJJK}\left[J(J+1)\right]^4 K^2 + {}^{(i)}M_{JJJKK}\left[J(J+1)\right]^3 K^4 \\
&+ {}^{(i)}M_{JJJKK}\left[J(J+1)\right]^2 K^6 + {}^{(i)}M_{JKKKK}\left[J(J+1)\right]K^8 + {}^{(i)}M_K K^{10} \\
&+ {}^{(i)}N_J\left[J(J+1)\right]^6 + {}^{(i)}N_{JJJJK}\left[J(J+1)\right]^5 K^2 + {}^{(i)}N_{JJJKK}\left[J(J+1)\right]^4 K^4 \\
&+ {}^{(i)}N_{JJJKKK}\left[J(J+1)\right]^3 K^6 + {}^{(i)}N_{JJKKKK}\left[J(J+1)\right]^2 K^8 + {}^{(i)}N_{JKKKKK}\left[J(J+1)\right]K^{10} + {}^{(i)}N_K K^{12}
\end{aligned}
$$

$$
\begin{aligned}
\begin{pmatrix} s \\ a \end{pmatrix}\langle v,J,K|H/hc|v,J,K\pm3\rangle\begin{pmatrix} a \\ s \end{pmatrix} = {}&\left\{\left[\alpha+\alpha_J(J(J+1))+\alpha_{JJ}(J(J+1))^2\right]\times(2K\pm3)+\left[\alpha_K+\alpha_{JK}(J(J+1))\right]\right. \\
&\left.\times\left[K^3+(K\pm3)^3\right]+\alpha_{KK}\left[K^5+(K\pm3)^5\right]\right\}F_{\pm3}
\end{aligned}
$$

$$(\quad)+{}^{(i)}\eta_K$$

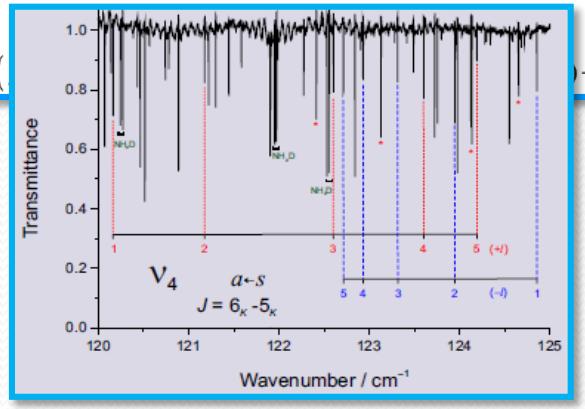

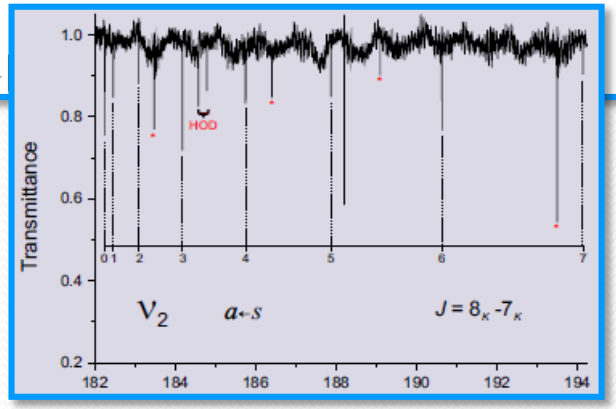

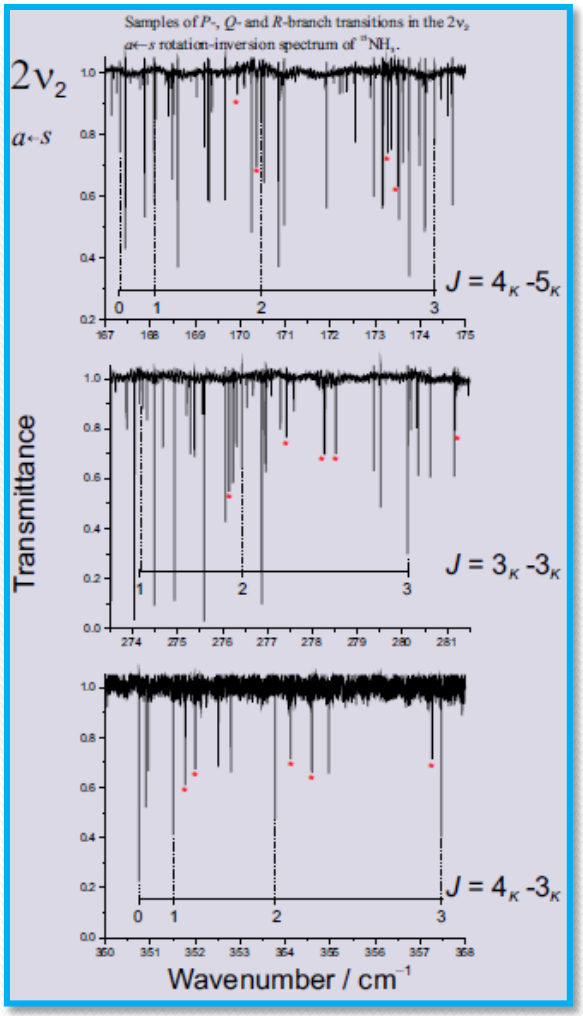

Synchrotron enabled spectroscopic study of formic acid and C-13 enriched acetylene

A. Predoi-Cross[a] M. Herman[b], G. Di Lonardo[c], L. Fusina[c]

[a]*Department of Physics and Astronomy, University of Lethbridge, Lethbridge Canada;* [b]*Laboratoire de Chimie Quantique et Photophysique, Université Libre de Bruxelles, Bruxelles, Belgium;* [c]*Dipartimento di Chimica Industriale "Toso Montanari", Università di Bologna, Viale Risorgimento 40136 Bologna, Italy*

Spectroscopic Goals for this study

- Formic acid (HCOOH), the simplest organic acid, exists in two rotameric form, *cis* and *trans* with respect to the relative position of the two hydrogen atoms.
- It was detected in the interstellar medium in 1971 and in the upper troposphere
- We report the observation and the analysis of the FIR spectrum of *trans*-HCOOH recorded under high resolution and very long path length. The observation is restricted to the *trans* rotamer, since in the adopted experimental conditions the weak transitions of the *cis* rotamer can be observed only below 40 cm^{-1}, outside the low wavenumber limit of the present recording, 62 cm^{-1}.
- Apart from early pioneering works, during the last 20 years the infrared spectrum of $^{13}C_2H_2$ has been the subject of several investigations
- In this study we have extended up to $\nu_{tot} = 4$ the previous observations of the bending states by means of spectra recorded at higher resolution and dynamical detection range, covering a larger spectral region by means of different experimental setups.
- Some results obtained from "band by band" analysis for several excited bending states have been already reported but now are included in a global fit that provides the molecular constants.

Detail of the far-infrared spectrum of trans-HCOOH in the region 92.94–93.12 cm^{-1} showing the ^{r}Q branch K_a 22-21.

Experimental conditions: pressure 66.66 Pa, and path length 72 m.

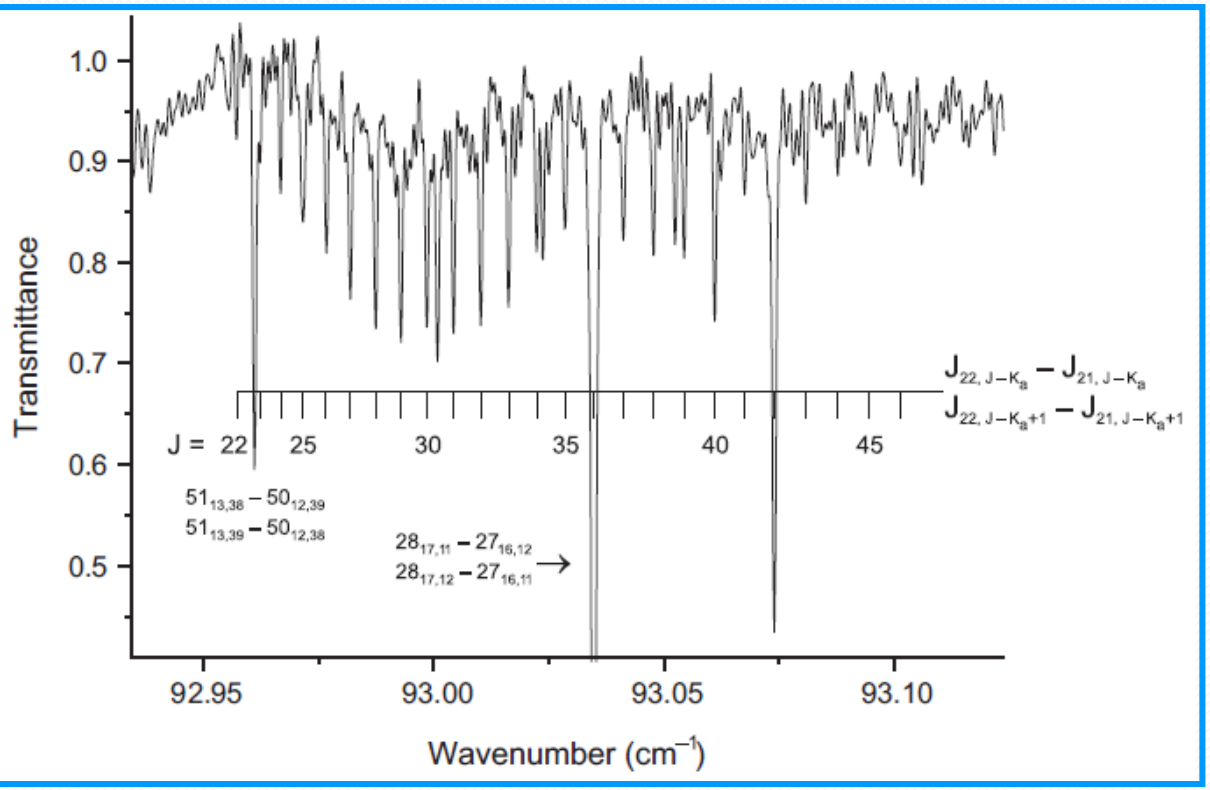

Spectroscopic parameters for the ground state of trans-HCOOH

parameters		This work
B_z	MHz	77512.226067(141)
B_x	MHz	12055.1047160(152)
C_y	MHz	10416.1139625(144)
Δ_J	kHz	9.9940848(253)
Δ_{JK}	kHz	−86.2211257(315)
Δ_K	kHz	1702.26776(314)
δ_J	kHz	1.94858375(559)
δ_K	kHz	42.776279(836)
Φ_J	Hz	0.0125585(155)
Φ_{JK}	Hz	0.12809(124)
Φ_{KJ}	Hz	−10.66818(470)
Φ_K	Hz	120.6862(266)
ϕ_J	Hz	0.00587594(454)
ϕ_{KJ}	Hz	0.079524(932)
ϕ_K	Hz	15.8356(647)
L_J	mHz	−0.00003914(233)
L_{JJK}	mHz	0.002073(443)
L_{KJ}	mHz	−0.3921(240)
L_{KKJ}	mHz	2.0342(682)
L_K	mHz	−12.6775(736)
l_J	mHz	−0.000018472(918)
l_{JK}	mHz	−0.001189(226)
l_{KJ}	mHz	0.1668(210)
l_K	mHz	−11.498(774)
P_{JJK}	μHz	−0.0001693(220)
P_{KKJ}	μHz	0.02051(224)
P_{KKKJ}	μHz	−0.1240(177)
P_K	μHz	1.2421(405)
Number of fitted data		7395
Standard deviation of an obse		1.08

Portion of the infrared spectrum of $^{13}C_2H_2$ in the FIR region showing *Q*-branch transitions of a vibrational band.

Experimental conditions: pressure=364 Pa; path length= 72.0 m; resolution=0.00096 cm^{-1}.

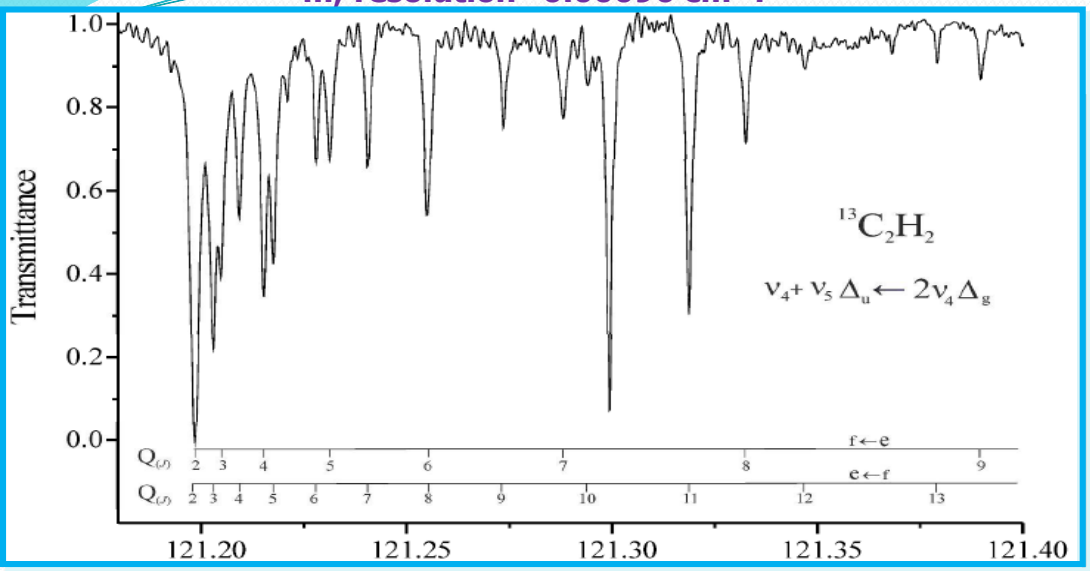

Portion of the infrared spectrum of $^{13}C_2H_2$ in the 500 cm^{-1} region showing *Q*-branch transitions.

Experimental conditions: pressure =364 Pa; path length=72.0 m; resolution= 0.002 cm^{-1}.

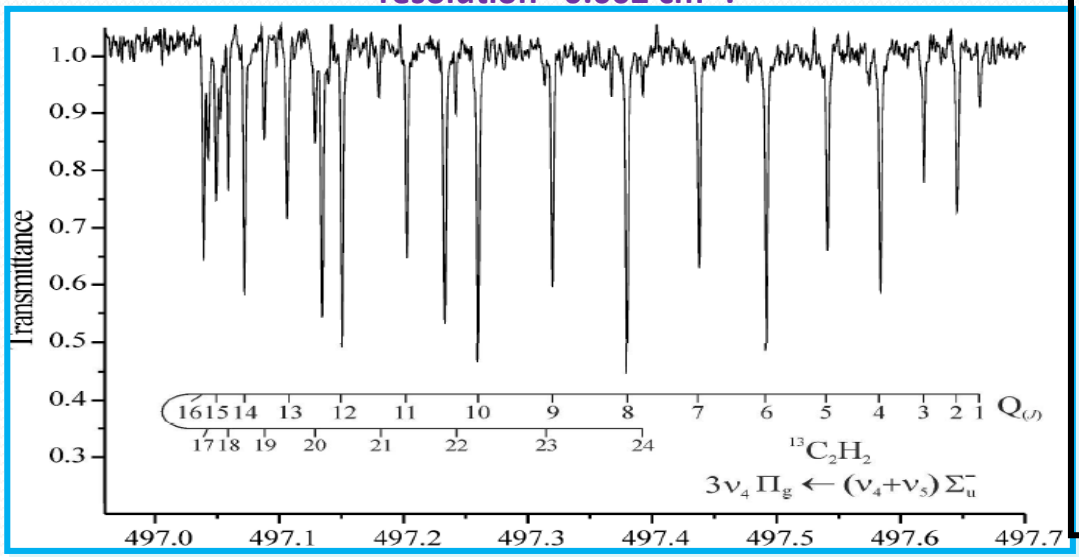

Sample of Spectroscopic Parameters (in cm^{-1}) for $^{13}C_2H_2$ Resulting from the Simultaneous Fit of all Sub-bands Involving Levels up to $v_4 + v_5 = 3$.

Parameter				Parameter			
ω_4^0		600.0665654	(349)	y_4^{44}		− 0.00610822	(552)
ω_5^0		727.1981581	(306)	y_4^{45}		0.007513	(121)
x_{44}^0		2.9964670	(229)	y_4^{55}		0.088473	(699)
x_{45}^0		− 2.415569	(571)	y_5^{44}		0.060248	(182)
x_{55}^0		− 2.3025686	(212)	y_5^{45}		− 0.041248	(462)
y_{444}^0		0.01635771	(466)	y_5^{55}		− 0.00609597	(468)
y_{555}^0		0.01301684	(453)	r_{45}^0		− 6.410785	(280)
y_{455}^0		0.095427	(235)	r_{45}^J	$\times 10^3$	0.1811782	(589)
y_{445}^0		− 0.0275539	(625)	r_{45}^{JJ}	$\times 10^9$	− 3.534	(129)
g_{44}^0		0.8146064	(151)	r_{45}^{JJJ}	$\times 10^{12}$	0.8951	(337)
g_{45}^0		6.649255	(568)	r_{445}		0.188728	(197)
g_{55}^0		3.4490997	(129)	r_{455}		− 0.0761305	(731)
B_0		1.119574352	(174)	γ^{44}	$\times 10^5$	− 6.65551	(909)
α_4	$\times 10^3$	− 1.031341	(141)	γ^{45}	$\times 10^5$	− 27.3300	(496)
α_5	$\times 10^3$	− 1.9303064	(945)	γ^{55}	$\times 10^5$	− 9.93414	(342)
γ_{44}	$\times 10^5$	0.29817	(455)	γ_4^{44}	$\times 10^5$	0.10761	(288)
γ_{45}	$\times 10^5$	4.2885	(476)	γ_4^{45}	$\times 10^5$	0.71440	(248)
γ_{55}	$\times 10^5$	1.77818	(458)	γ_4^{55}	$\times 10^5$	− 8.7671	(705)
γ_{445}	$\times 10^5$	0.65795	(338)	γ_5^{44}	$\times 10^5$	− 1.12413	(718)
γ_{455}	$\times 10^5$	2.5779	(231)	γ_5^{45}	$\times 10^5$	5.3926	(497)

(B) Assignment of Far-Infrared Laser Lines of O-17 Methanol by Synchrotron FTIR Spectroscopy and Laser Frequency Measurements

R.M. Lees, M. Jackson, G. Moruzzi, Adriana Predoi-Cross, B.E. Billinghurst

[a]Centre for Laser, Atomic and Molecular Sciences (CLAMS) and Physics Department,University of New Brunswick, Saint John, NB, Canada; [b]Department of Physics, Central Washington University, Ellensburg, WA 98926; [c]Departimento di Fisica "Enrico Fermi" dell'Università di Pisa, Pisa, Italy; ;[d]Department of Physics and Astronomy, University of Lethbridge, Lethbridge, AB, Canada; [e]Canadian Light Source Inc., University of Saskatchewan, Saskatoon, Canada

Methanol is found throughout the universe in a wide variety of astronomical sources from giant interstellar clouds to dense hot cores where protostars are forming, down to comets in our own solar system.

Methanol is a primary issue for radio astronomers, as its dense and complex spectrum extends across all of the frequency bands that will be probed by the new telescopes.

Currently, sparse experimental data exist on the spectra and molecular Analysis of synchrotron FTIR spectra of $CH_3{}^{17}OH$ has revealed new assignments for a number of optically pumped far-infrared laser lines from the $CH_3{}^{17}OH$ isotopologue of methanol, with definitive confirmation provided by recent accurate measurements of the laser frequencies.

Laser Based Spectroscopic Studies of Acetylene

Table. Assignments for FIR laser lines of the $CH_3{}^{17}OH$ isotopologue of methanol optically pumped in the CO-stretching band by CO_2 laser lines

CO_2 Line ± Offset (MHz)[a]	λ_{laser} (μm)	ν_{laser}[b] (cm^{-1})	IR Pump[c] (v_t, K, J)^v TS	FIRL Assignment (v_t',K',J')$^{v'}$ → (v_t'',K'',J'')$^{v''}$	ν_{calc}[d] (cm^{-1})	Ref.
9*P*14+21	278.655	35.88662	$R(0,3,22)^{co}$ E_1	$(0,3,23)^{co}$ → $(0,3,22)^{co}$	35.8864	[5,6]
[1052.19625]	562.331	17.78312	[1052.19626]	→ $(0,2,23)^{co}$	17.7828	[5,6]
	186.575	53.59764		→ $(0,2,22)^{co}$	53.5976	[5,6]
9*P*18+25	319.343	31.31428	$R(0,2,19)^{co}$ E_2	$(0,2,20)^{co}$ → $(0,2,19)^{co}$	31.3143	[5,6]
[1048.66164]	642.707	15.55920	[1048.66166]	→ $(0,1,20)^{co}$	15.5592	[5,6]
	214.664	46.58445		→ $(0,1,19)^{co}$	46.5847	[6]
9*P*32+17	227.945	43.87016	$R(0,5,9)^{co}$ E_1	$(0,5,10)^{co}$ → $(0,4,9)^{co}$	43.8707	[5,6]
[1035.47418]	353.739	28.26940	[1035.47417]	→ $(0,4,10)^{co}$	28.2701	[5,6]
10*R*40-10	357.319	27.98620	$P(0,0,19)^{co}$ A	$(0,0,18)^{co}$ → $(0,0,17)^{co}$	27.9863	[5,6]
[987.61985]	506.915	19.72718	[987.61984]	→ $(0,1^+,17)^{co}$	19.7272	[5,6]

[a] The wavenumber of the CO_2 pump line plus the reported offset is shown underneath in brackets, using the conversion factor 29979.2458 MHz/cm^{-1}.

[b] Wavenumber of the FIR laser line calculated from the reported FIR laser frequency.

[c] The experimental wavenumber for the IR pump transition as measured in the FTIR synchrotron spectrum is shown underneath in brackets.

[d] FIR laser wavenumber predicted from IR/FIR transition combination loops or from ground and excited state term values determined from the spectroscopic FIR and IR transition wavenumbers.

Fig. Energy level and transition diagram for the FIRL system pumped by the 9P14 CO_2 line at 21 MHz offset, with the experimental wavenumbers for the three frequency-measured FIR laser lines. The observed spectroscopic wavenumbers are shown for the IR and FIR transitions, and term values from the Ritz analysis are given for the lower v_t = 0, 3E1 ground-state levels.

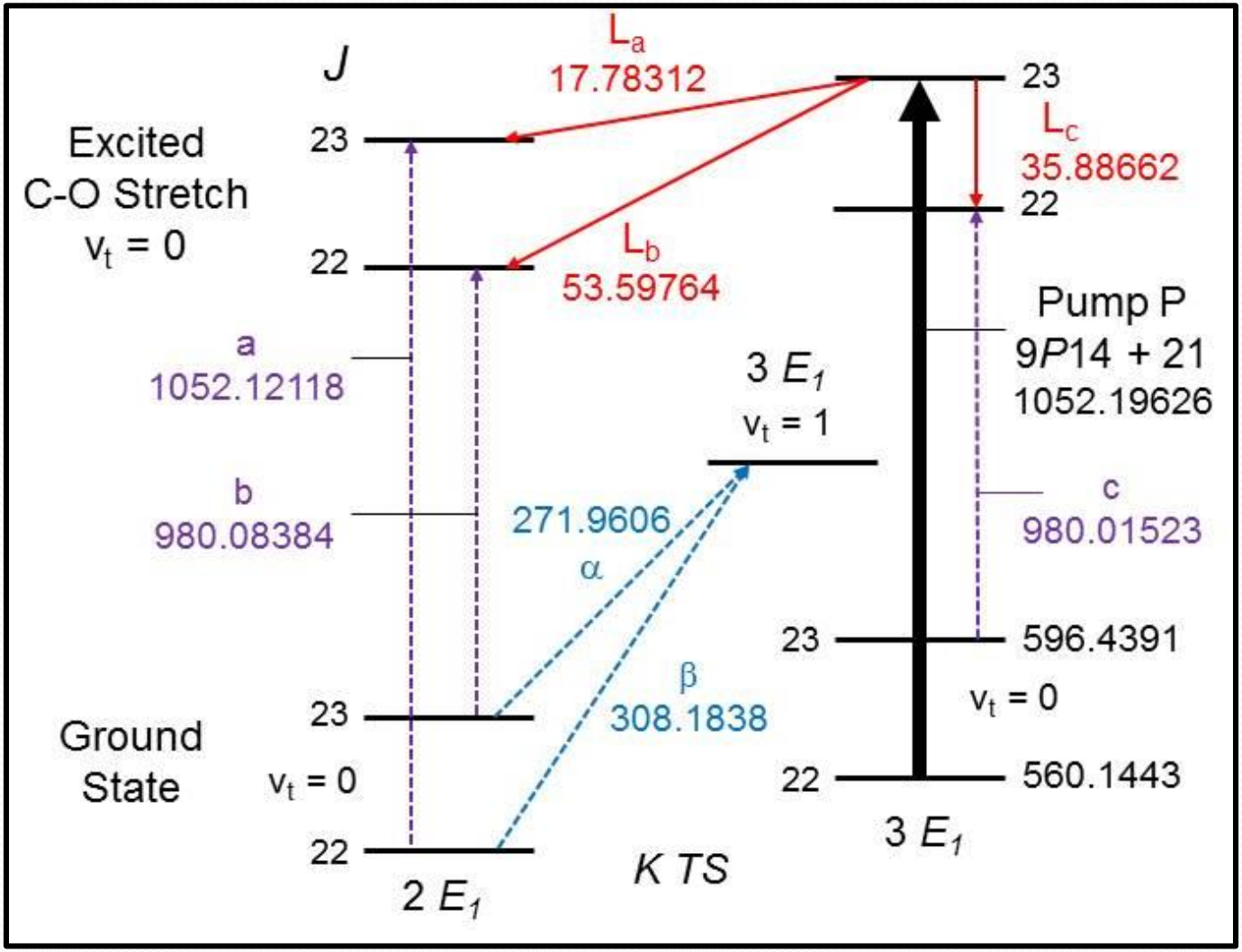

Laser Based Spectroscopic Studies

Low pressure line shape study of N_2-perturbed acetylene transitions in the $\nu_1+\nu_3$ band over a range of temperatures

- Six nitrogen-perturbed transitions of acetylene within the $\nu_1+\nu_3$ band absorption band have been recorded using a three-channel diode laser spectrometer.
- The goal being an improved understanding of both broadening and **narrowing** effects of low-pressure acetylene under the influence of nitrogen gas. We have examined C_2H_2 spectra using a **hard collision** Rautian profile over a range of five temperatures (213–333 K) and five pressures (5–40 Torr).
- From these fits we have obtained the N_2-broadening and narrowing coefficients of C_2H_2 and examined their temperature dependence.
- The experimentally measured narrowing coefficients have been used to estimate the nitrogen **diffusion coefficients** (D_{12}) and are presented within.
- The broadening coefficients and corresponding temperature dependence exponents have also been compared to that of calculations completed using a classical impact approach on an ab initio potential energy surface.

Comparison of classically calculated and experimentally determined N_2-broadening coefficients for three different temperatures.

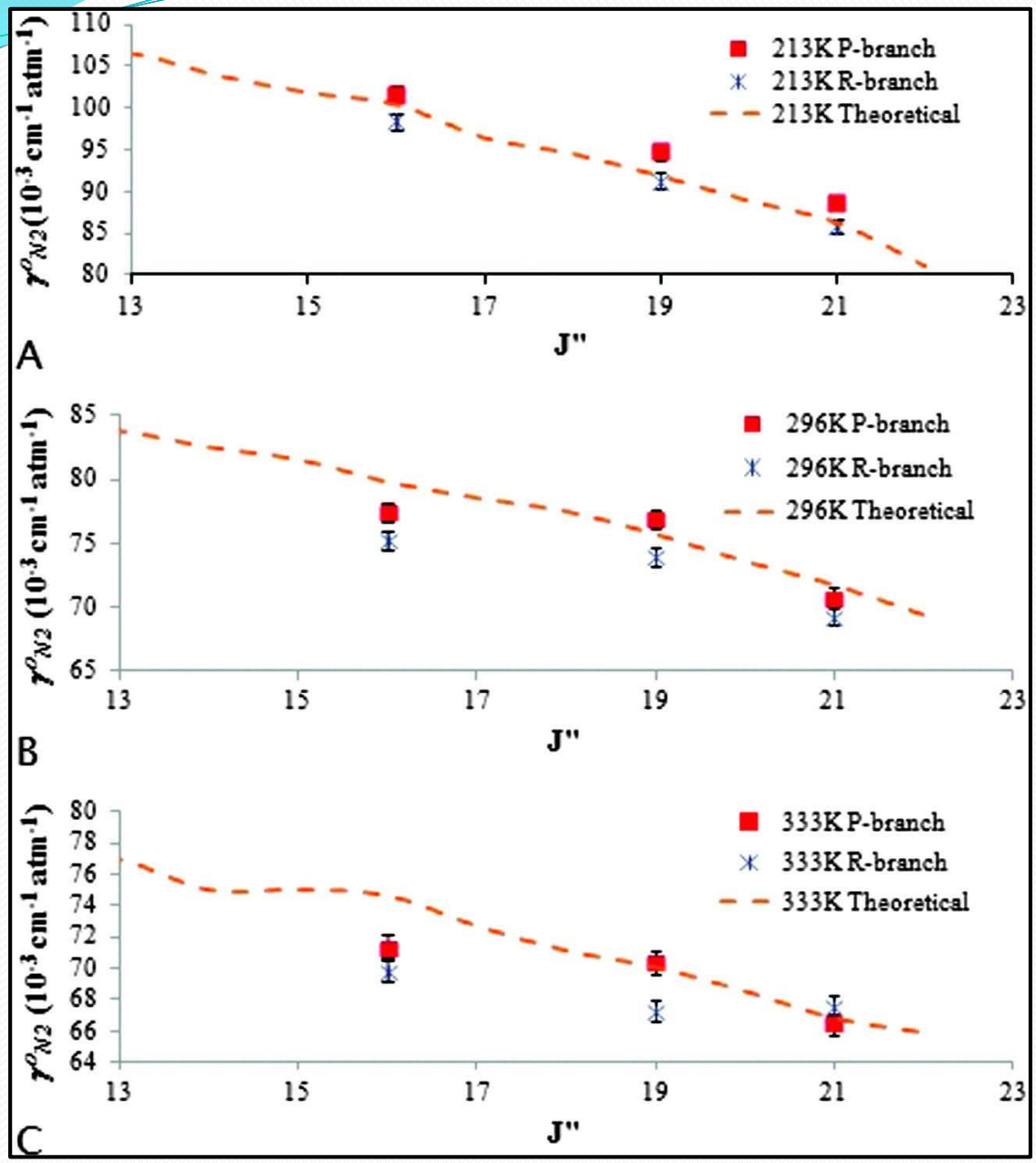

We have observed good agreement between our theoretical and experimental results.

Temperature dependence exponents, n.

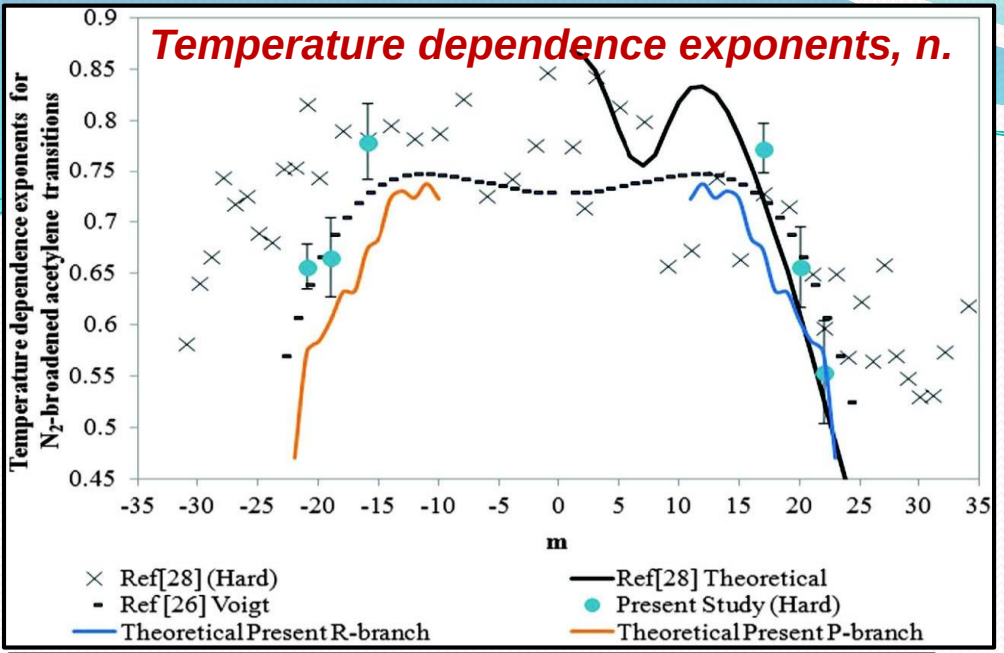

Narrowing temperature dependence coefficient

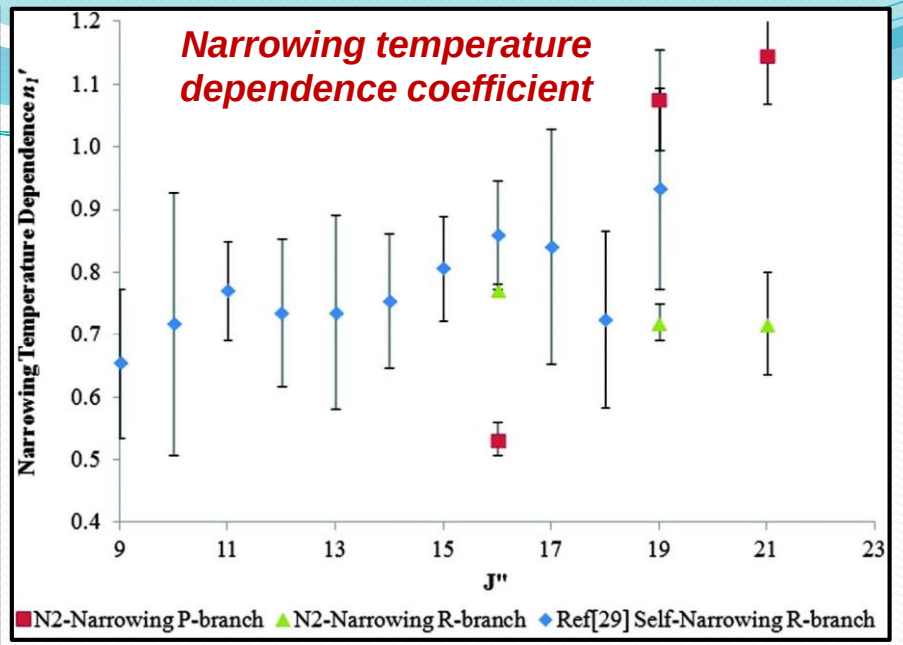

Estimated diffusion coefficients.

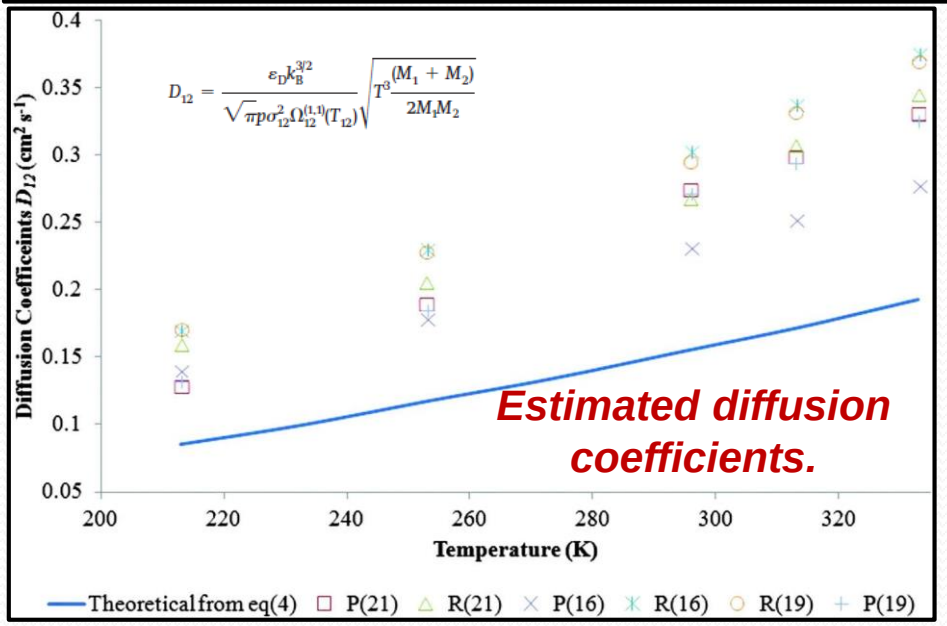

Comparison of the N_2-narrowing coefficients obtained at 296 K to previous work.

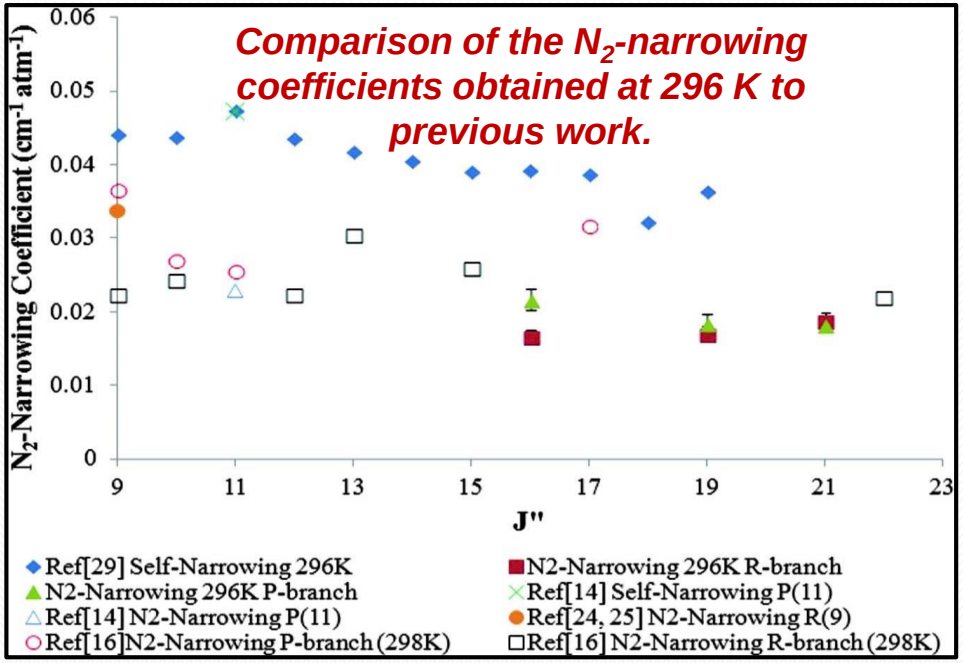

➢This study has been published in *C. Povey, M. Guillorel-Obregon, A. Predoi-Cross, S.V. Ivanov, O.G. Buzykin, F. Thibault, Can. J. Phys. 91: 896–905 (2013)* .

Line Shape and Doppler Thermometry Studies Using Acetylene Transitions in the $\nu_1+\nu_3$ Band

- The $\nu_1+\nu_3$ band of acetylene, with ν_1 as the symmetric CH stretch and ν_3 as the anti-symmetric stretch is a strong absorption band compared to other nearby absorption bands.
- It provides a good test case for measurements of fundamental physical constants such as the optical determination of the Boltzmann constant.
- The accepted value for the k_B published by the Committee on Data for Science and Technology (CODATA) is 1.3806488×10^{-23} JK^{-1} with a relative uncertainty of 9.1×10^{-7}.
- One of the recent methods of measuring k_B is the laser spectroscopy using Doppler-width thermometry approach, which was used in our study.

Experimental Details

The experiment is based on measuring ro-vibrational absorption features of C_2H_2 gas inside a temperature and pressure controlled cell maintained at thermal equilibrium. The width at half-maximum of the absorption line is dominated by the Doppler width due to the molecular velocity distribution along the laser beam at low gas pressure.

The Doppler width of a spectral absorption line recorded in a cell is related to the equilibrium temperature and Boltzmann constant as it is shown in:

$$\gamma_D = \frac{2\nu_0}{c}\sqrt{\frac{2k_B T \ln 2}{m_E}} \quad \Rightarrow \quad k_B = \left(\frac{\gamma_D}{\nu}\right)^2 \left(\frac{Mc^2}{2\ln(2)T}\right)$$

where D is the Doppler broadening, M is the mass of the gas particle, c is the speed of light, T is temperature, and ν is the line position.

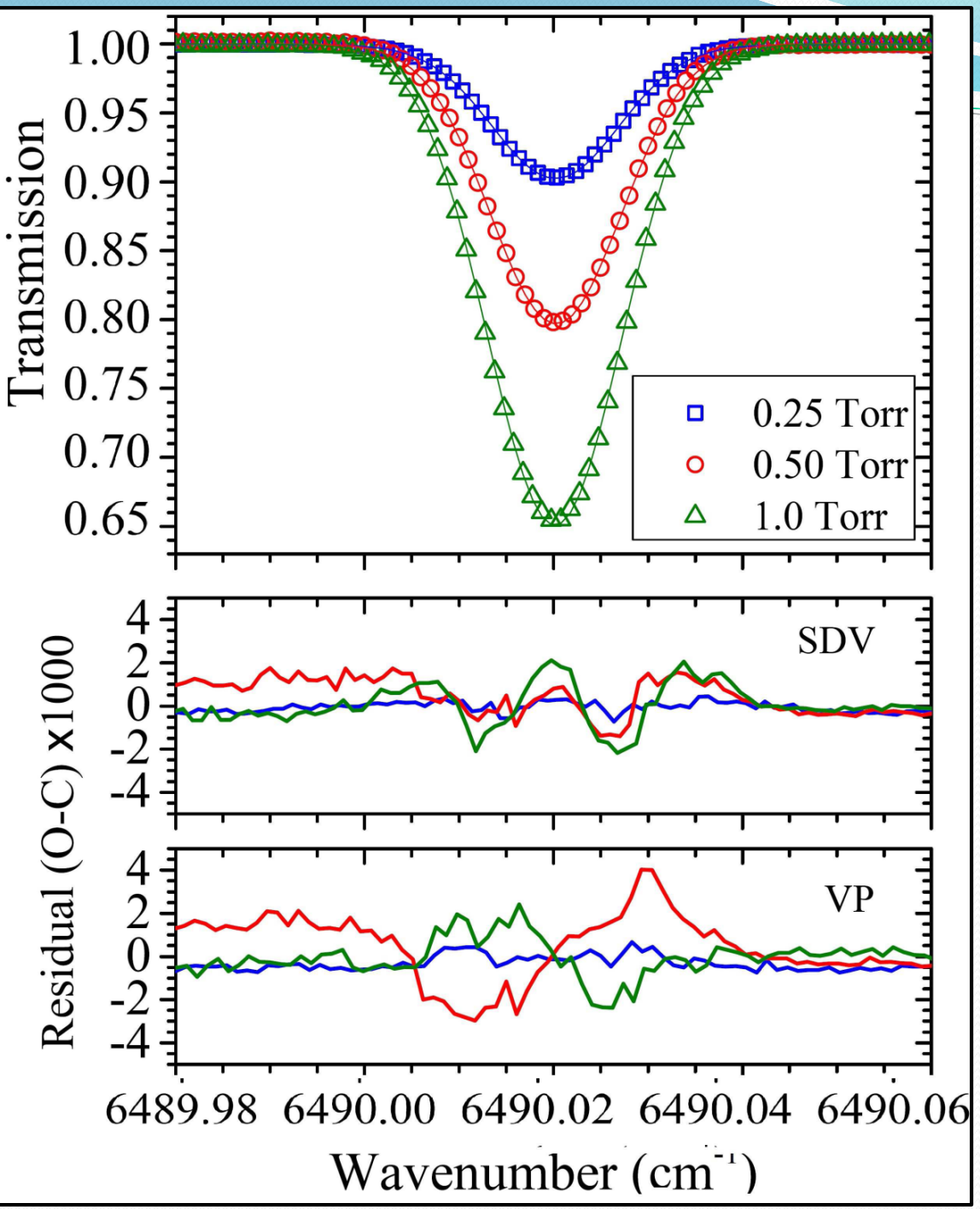

The transmission spectrum of the P(25) line at pressures 0.25-1 Torr and 295.78 K.

- In this study, we have performed a line-shape analysis of acetylene at room temperature and low gas pressures considering the Voigt (VP) and Speed Dependent Voigt (SDV) profiles.

- We can conclude that our limiting factor was not the signal to noise ratio but the line-shape model used and the determination of the parameters as we obtained more precise value for k_B using SDV model.

Analysis Method

- We fitted the line position, intensity, broadening and Doppler width while fixing the self-shifting values to the highly accurate values determined by our group.
- We determined the self-broadening by setting it to specific values and then fitted for the Doppler width to obtain a pressure dependence relationship that could be used to obtain the corrected self-broadening value.
- To determine a precise value for the self-broadening coefficient we calculated the standard deviation of all Doppler width values over the pressure range for a single self-broadening value and plotted the results.
- We then fitted these points to a quadratic function and calculated the minimum based on the first derivative of the equation of best fit.
- The minimum value obtained served to be our optimum self-broadening value. We used these values to obtain the Doppler width where it was constant with pressure. The self-broadening value & Doppler width were plotted on a three dimensional surface with the pressure on one plane.
- The Doppler width value should be constant with pressure as it is only a function of physical constants. Therefore the correct self-broadening coefficient should allow for the retrieval of a constant Doppler width. Using this Doppler width, we were able to calculate k_B.

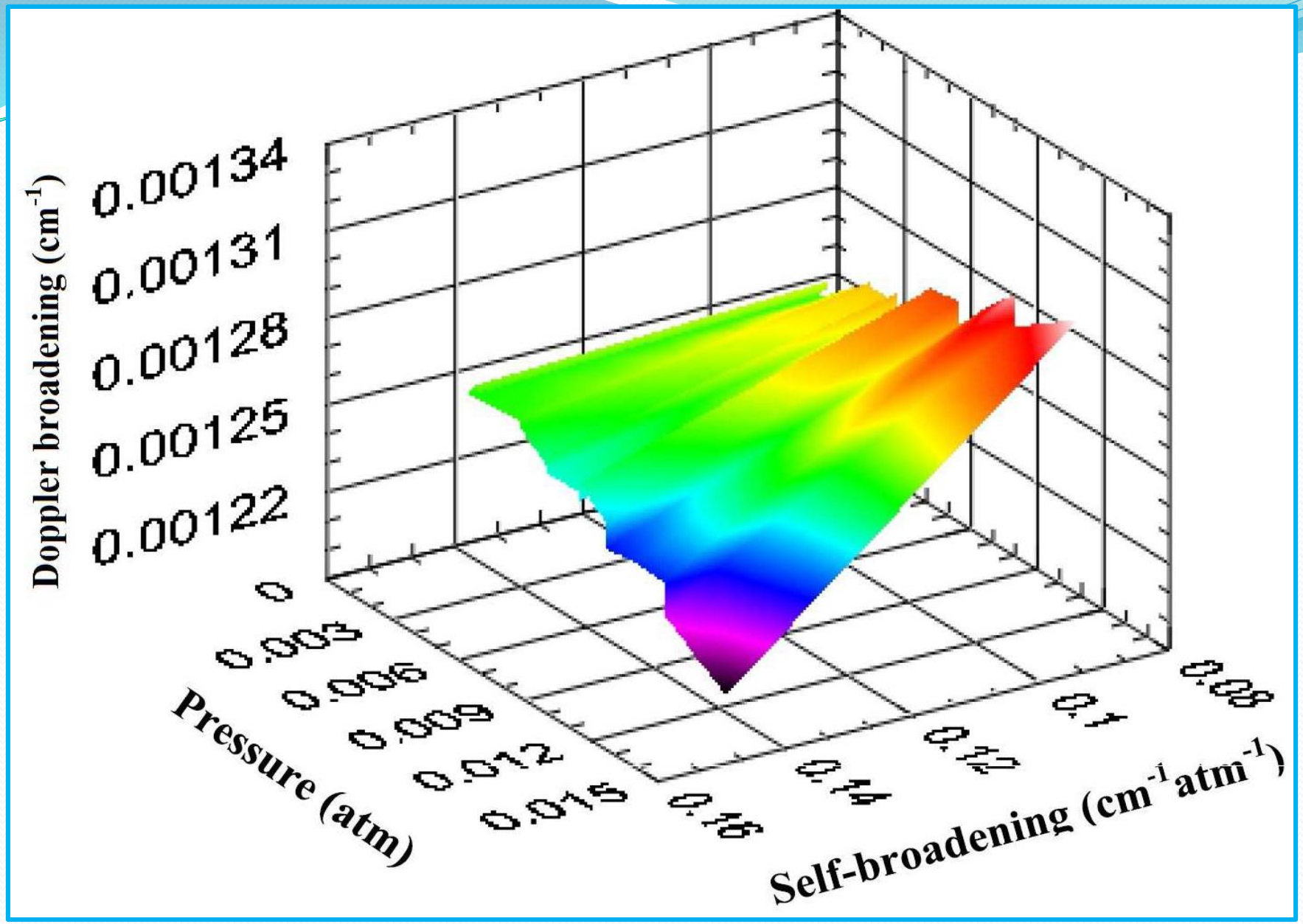

3-D Surface plot visualization of where Doppler broadening remained constant across all pressures for a single self-broadening value.

Statistical error analysis

- Using statistical error analysis, most of the uncertainty in this measurement was due to the line-shape fitting and temperature measurements. The uncertainty in the modelling of collisional effects was limited by our knowledge on the fitting parameters such as self-broadening, Doppler width and parameter *q* and thus parameters *m* and *n* in the SDV model.

$$\frac{\delta_{K_B}}{K_B} = \sqrt{4\left(\frac{\delta_{\gamma_D}}{\gamma_D}\right)^2 + 4\left(\frac{\delta_\nu}{\nu}\right)^2 + \left(\frac{\delta_T}{T}\right)^2}$$

Error of Doppler width (γ_D): 1.47×10^{-6} cm^{-1}
Error of position (ν): $0.0000165\ cm^{-1}$
Error of temperature (T): 1.69×10^{-5} K
Relative error of k_B=3.21×10^{-5} JK^{-1}

- The accurate calculated value for the Boltzmann constant using Doppler thermometry in our experiment was 1.38064906×10^{-23} JK^{-1} with relative uncertainty of 3.21×10^{-5} at low pressure for SDV model and 1.38065243×10^{-23} with relative uncertainty of 5.8×10^{-4} for VP.

- This study is published as *Hashemi, R.; Povey, C.; Derksen, M.; Naseri, H.; Garber, J.; Predoi-Cross, A. Journal of Chemical Physics. 2014, Vol. 141 Issue 21, p1-7.*

CONCLUSIONS

The primary beneficiaries of laboratory spectroscopic studies presented here are the atmospheric and astrophysical community.

The spectroscopic results of our laboratory investigations enable more accurate modeling of infrared radiative transfer in the atmosphere of Earth and other planetary bodies.

The spectroscopic parameters will also be valuable for improving the understanding of past and future infrared observations of planets and for designing instrumentation for future space missions not only to explore the outer planets, but also to study extra-Solar planetary systems.

"We are a way for the cosmos to know itself. "
(Carl Sagan)

References

[1] S. Yu, J.C. Pearson, B.J. Drouin, K. Sung. O. Pirali, M. Vervloet, M.-A. Martin-Droumel, C.P. Endres, T. Shiraiashi, K. Kobayashi, F. Matsushima, *Submillimeter-wave and far-infrared spectroscopy of high-J transitions of the ground and v_2=1 states of ammonia,* J. Chem. Phys. **133** 174317 (2010).

[2] M. Carlotti, A. Trombetti, B. Velino, J. Vrbancich, *The rotation-invesion spectrum of $^{15}NH_3$*, J. Mol. Spectrosc. **83** 401 (1980).

[3] S. Urban, S. Klee and K.M.T. Yamada, *Ground-state ro-inversional transitions of (NH3)-N-15 in the far-infrared region*, J. Mol. Spectrosc. 168 384 (1994).

[4] G. Di. Lonardo, L. Fusina, A. Trombetti, and I.M.Mills, *The v_2, $2v_2$, $3v_2$, v_4 and v_1+ v_4 bands of $^{15}NH_3$* J. Mol. Spectrosc. **92** 298 (1982).

Acknowledgements

The spectroscopy group at University of Lethbridge was funded by NSERC, Canada. The research described in this paper was performed at the Canadian Light Source, which is supported by NSERC, NRC, CIHR, and the University of Saskatchewan.

Thank you!